Supplementary Data

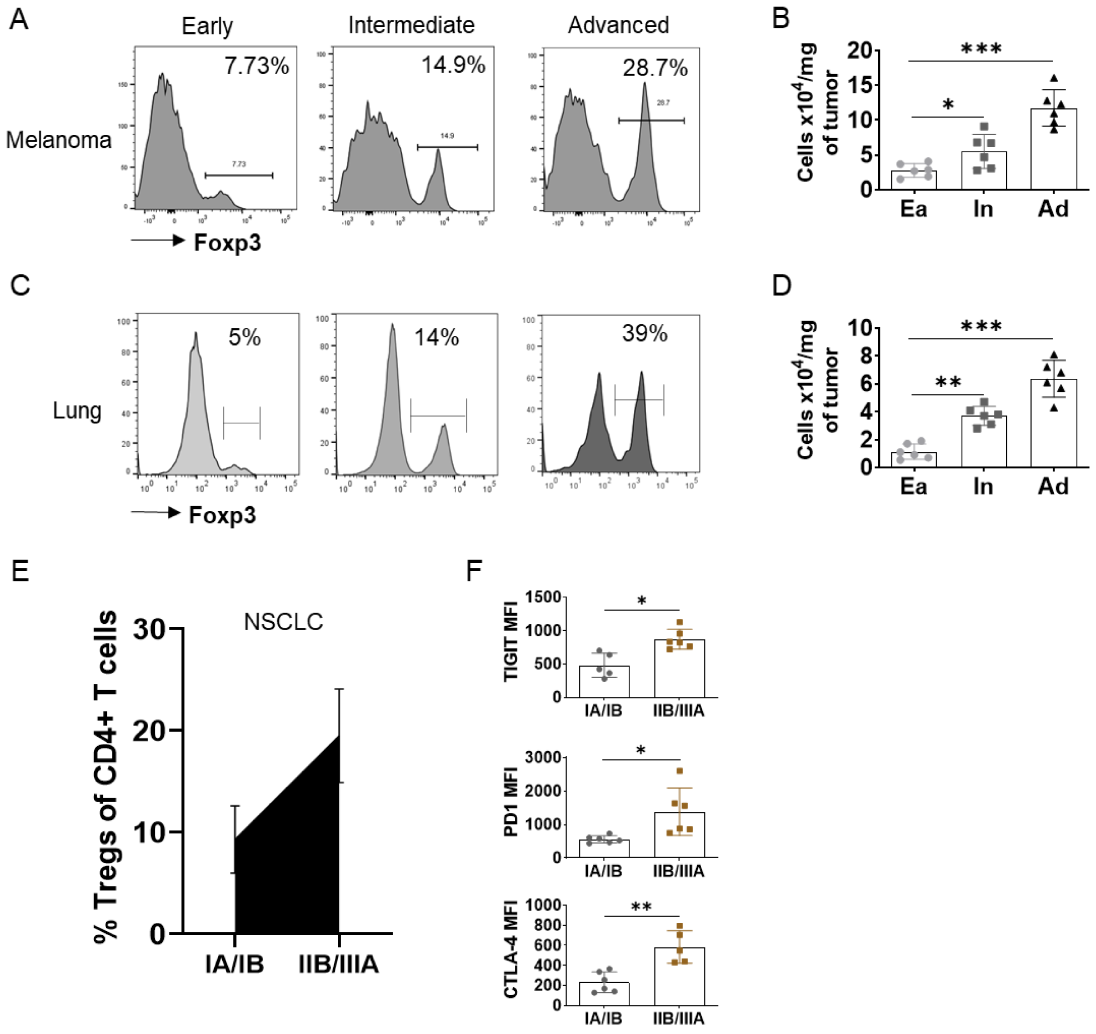

Fig. S1. Accumulation of Tregs correlates with severity of dysfunctional phenotype exhibited by tumor-associated CD8+ T cells. The proportion of Tregs was evaluated by flow cytometry in tumors resected from B16-F10 melanoma or KP lung tumor-bearing mice at early, intermediate, or advanced disease stages. (A-D) Representative histograms (A, C), and summary of absolute cell counts per milligram of tumor (B, D) for Tregs in melanoma and lung tumor as evaluated by the proportion of Foxp3+ cells within gated viable CD45+CD3+CD25hi cells in the tumors. (E) Percent Tregs of total CD4+ T cells in non-small cell lung cancer (NSCLC) patient tumor tissues that were evaluated at indicated tumor stages. Parallel analysis was conducted to determine the phenotype of CD8+ T cells. (F) Summary for the expression of TIGIT (top), PD-1 (middle), and CTLA-4 (bottom) on CD8+ T cells in NSCLC patient tumors as determined by median fluorescent intensity (MFI). Data are representative of 6 mice per group (A and C) or 5-6 patient samples per disease stage (E). * indicates p-value < 0.05, ** p-value < 0.01, *** p-value < 0.001. Ea; Early disease stage, In; Intermediate disease stage, Ad; Advanced disease stage.

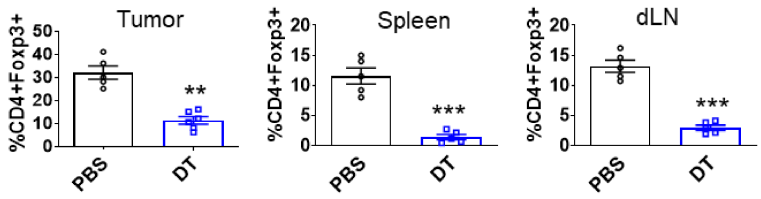

Fig. S2. Treg depletion efficiency in Diphtheria toxin-treated Foxp3^{DTR} mice. B16-F10 melanoma resected from Foxp3^{DTR} mice that were treated with Diphtheria toxin (DT) or with PBS were analyzed by flow cytometry to determine Treg depletion efficiency. Shown is the percent of CD4+CD25hiFoxp3+ Tregs in the tumor (left), spleen (middle), and draining lymph nodes (right). dLN; draining lymph nodes. ** indicates p-value < 0.01, *** p-value < 0.001.

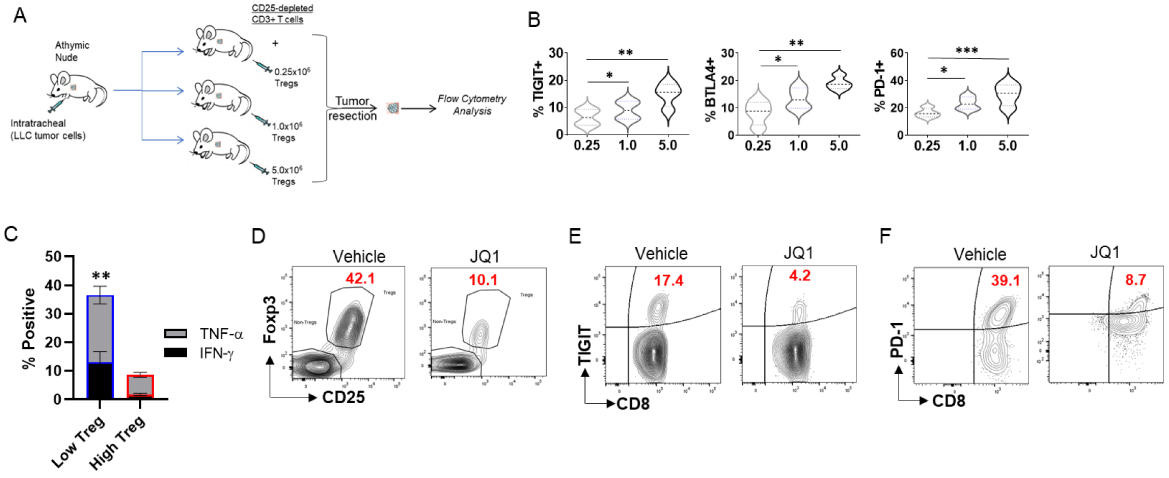

Fig. S3. Higher Tregs frequencies in the tumor bed correlate with CD8+ T cell dysfunction in lung tumors. Athymic nude mice were orthotopically implanted with LLC-1 tumor cells after which they were adoptively transferred with CD25-CD3+ T cells mixed with graded numbers of CD4+CD25hi Tregs isolated from the spleen of wild-type (WT) B6 mice. Tumors were resected around day 30 post tumor inoculation for phenotypic analysis by flow cytometry and for in vitro stimulation assays. (A) Experiment schema. (B) Summary for the percent of TIGIT+ (left), BTLA+ (middle), and PD-1+ (right) CD8+ T cells in the tumors of mice under each T cell transfer condition. Tumor-infiltrating CD45+CD3+ T cells isolated from the tumors were stimulated for 6 hours with Cell Stimulation Cocktail plus protein transport inhibitor after which intracellular staining was conducted. (C) Percent of CD8+ T cells that expressed IFN-γ or TNF-α under low or high Treg transfer. KP mice with established tumors (150-200 mm^3) were treated with JQ1 for 4 weeks after which the phenotype of tumor-associated CD8+ T cells was evaluated by flow cytometry. (D) Representative zebra plot for the proportion of CD25+Foxp3+ Tregs within gated CD4+ T cells in the lung tumors of vehicle and JQ1-treated mice. (E) Representative zebra plots for the expression of TIGIT in tumor-associated CD8+ T cells from vehicle and JQ1-treated mice. (F) Representative zebra plots for the expression of PD-1 in tumor-associated CD8+ T cells from vehicle and JQ1-treated mice. Data in B and C are mean ± SEM of 5-6 mice per group. * indicates p-value < 0.05, ** p-value < 0.01, *** p-value < 0.001.

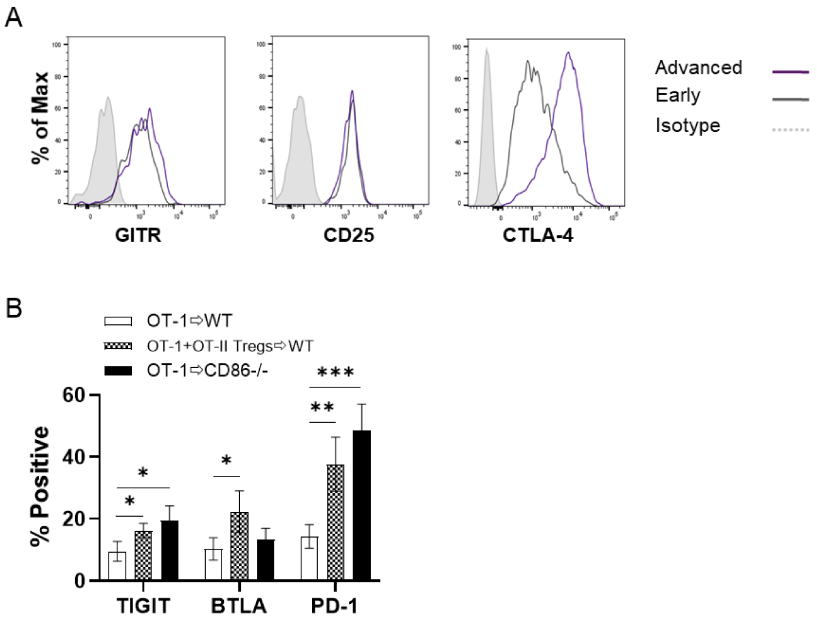

Fig. S4. Diminished co-stimulatory molecule availability through augmented Treg-expressed CTLA-4 underlies the establishment and sustenance of dysfunctional phenotype in tumor-associated CD8+ T cells. The phenotype of Tregs in the tumors of B16-F10 melanoma-bearing mice was evaluated. (A) Representative histograms for the expression of GITR (left), CD25 (middle), and CTLA-4 (right) on tumor-associated Tregs in early and advanced-stage disease. OT-1 CD8+ T cells alone or mixed with OT-II Tregs were injected into B16-F10 melanoma bearing CD45.1 congenic WT or CD86-/- mice. The phenotype of tumor-associated CD8+ T cells was assessed. (B) Percent TIGIT+ (left), BTLA+ (middle), and PD-1+ (right) in gated tumor-CD8+ T cells. Data is representative (A) or are mean ± SEM (B) of 5-6 mice per group. * indicates p-value < 0.05, ** p-value < 0.01, *** p-value < 0.001.

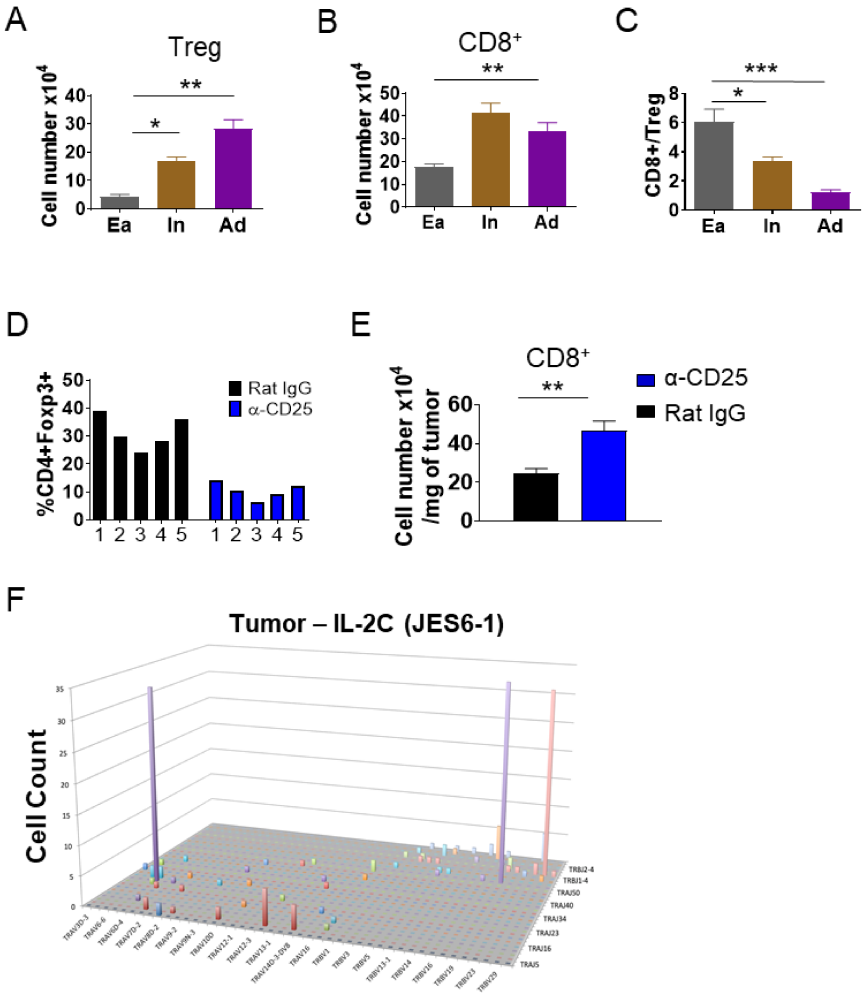

Fig. S5. The waning of CD8+ T cells as tumor progresses is rescued by Treg reduction in the tumor. B16-F10 melanoma tumors were resected at early (Ea), intermediate (In), and advanced (Ad) tumor stages and proportions of T cell subsets were quantified through flow cytometric analysis. Proportion of (A) Tregs and (B) CD8+ T cells per milligram of tumor. (C) CD8:Treg ratio. B16-F10 melanoma-bearing mice were treated for 2 weeks with α-CD25 antibody to deplete Tregs or Rat IgG Isotype antibody as controls after which tumors were resected tumors and evaluated for proportions of T cell subsets. (D) Frequency of CD4+Foxp3+ Tregs as a fraction of total CD4+ T cells and (E) Absolute cell number per milligram of tumor for CD8+ T cells in the tumors of control and treated mice. B6 mice with established B16-F10 tumors were treated with IL-2C (α-IL-2 antibody clone JES6-1) by intratumoral injection. The clonal diversity of CD8+ T cells isolated from tumors of these mice was assessed by TCR sequencing. (F) Representative 3-D graph showing the clonal distribution of the tumor-CD8+ T cells. Data are mean ± SEM of 5 mice per group (A-D) or representative of 3 biological replicates. * indicates p-value < 0.05, ** p-value < 0.01, *** p-value < 0.001.

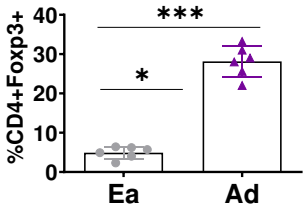

Fig. S6. Increased Treg proportions in advanced-stage melanoma. Tumors from B16-F10 melanoma-bearing B6 were resected and assessment of Treg proportions at early (Ea) and advanced (Ad) tumor stages was conducted by flow cytometry. Shown is percent of CD4+Foxp3+ Tregs within gated CD4+ cells. * indicates p-value < 0.05, *** p-value < 0.001.

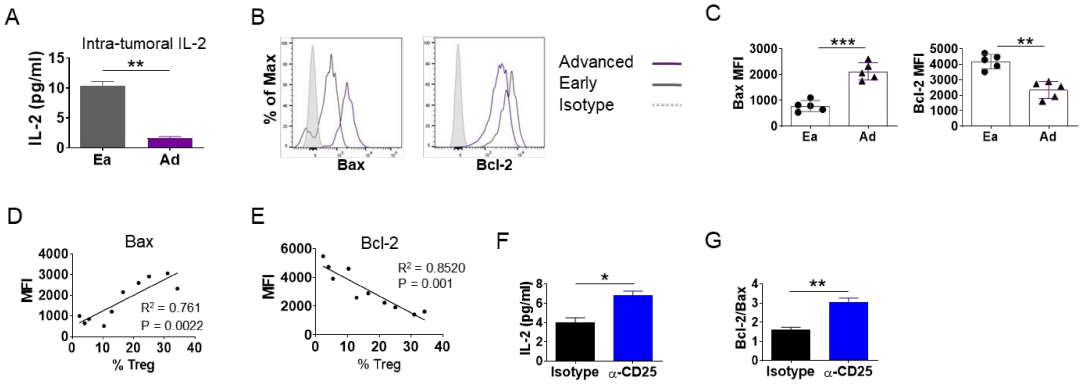

Fig. S7. Improved IL-2 availability and survival profile of tumor-associated CD8+ T cells accompany Treg-depletion in the tumor microenvironment. Lewis Lung carcinoma (LLC1) cell line was orthotopically implanted into B6 mice. Bronchoalveolar lavage fluid was collected from early (Ea) or advanced (Ad) stage tumors and analyzed by ELISA. (A) IL-2 concentration in the tumor-draining BAL fluids at indicated tumor stages. The phenotype of CD8+ T cells in these tumors was evaluated by flow cytometry. (B) Representative histograms and (C) Summary for the expression of Bax (left) and Bcl-2 (right). Treg proportions and CD8+ T cell phenotype were evaluated in LLC1 tumor tissues. (D, E) Correlation between % Tregs in tumors and expression levels of Bax (D) and Bcl-2 (E) as determined by median fluorescent intensity (MFI). BAL fluids were collected from the lungs of LLC tumor-bearing mice that were treated with α-CD25 or Rat IgG isotype as controls and subjected to cytokine analysis by ELISA. (F) IL-2 concentration in the tumor-draining BAL fluids. (G) Bcl2/Bax ratio in tumor-associated CD8+ T cells under each treatment condition as determined from MFI expression values. Data is representative (B) or are mean ± SEM (A, C, F, G) of 5-6 mice per group. * indicates p-value < 0.05, ** p-value < 0.01, *** p-value < 0.001.

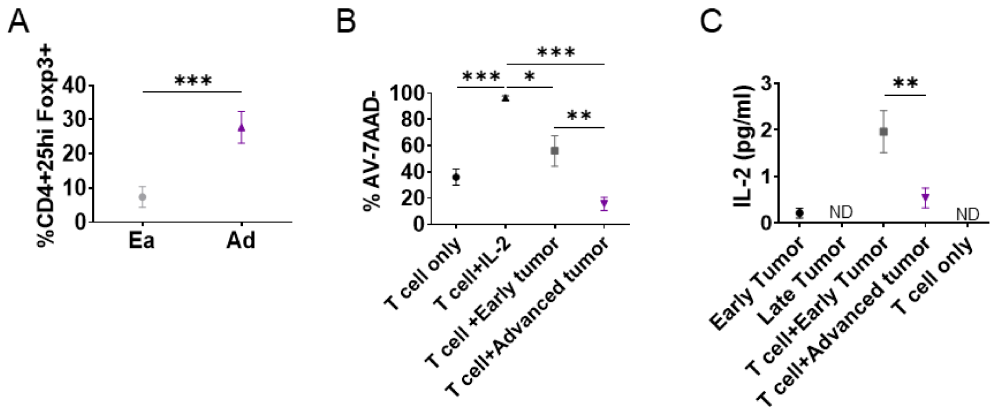

Fig. S8. Reduced viability of tumor-specific CD8+ T cells is coincident with limited IL-2 availability. Pmel-1 TCR transgenic T cells were injected into B16-F10 melanoma-bearing mice. 1-week post-transfer, the pmel-1 CD8+ T cells were sorted from tumor single-cell suspensions using Thy1.1-specific antibodies followed by 2-hours activation with hgp10025–33 peptide-pulsed APCs for two hours after which they were co-cultured with spheroids generated from early or late-stage tumors for 48 hours. (A) Percent of CD4+CD5hiFoxp3+ Tregs in a fraction of early or late tumors as assessed by flow cytometry. (B) Percent viability of pmel-1 CD8+ T cells in the co-cultures as indicated. T cell only cultures with and without IL-2 served as positive and negative controls, respectively. (C) Concentration of IL-2 in the supernatant of cultures as indicated. Data are mean ± SEM of 3 independent experiments. * indicates p-value < 0.05, ** p-value < 0.01, *** p-value < 0.001, and ND = Not detected.

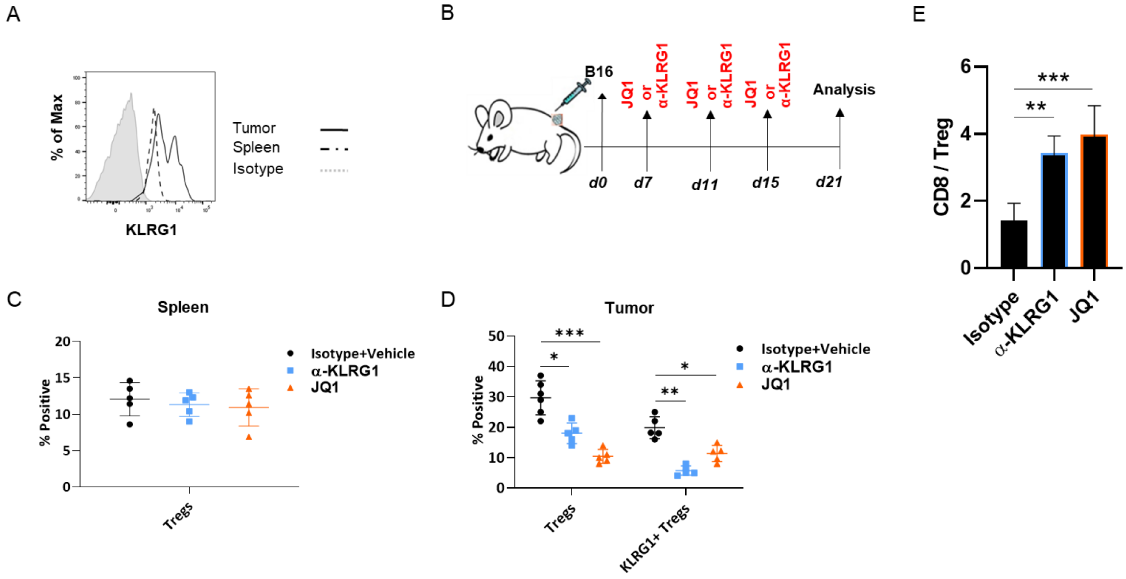

Fig. S9. Tumor-confined Treg targeting facilitates increased intratumoral CD8+ T cell to Treg ratio. (A) Representative histogram for the expression of KLRG1 on gated CD4+CD25hiFoxp3+ Tregs in the spleen or tumor of B16-F10 melanoma-bearing mice. Mice with established (~50 mm^3) B16-F1-melanoma were treated with either α-KLRG1 antibody or the bromodomain inhibitor JQ1 every 4 days from day 7 to day 15 post tumor inoculation. Control mice received Rat IgG isotype/vehicle. Tumors were resected at day 21 and analyzed for proportions of Tregs. (B) Schematics of the short-term *in vivo* drug treatment in B16-F10 inoculated mice. (C, D) Percent of cells positive for Treg markers (CD25hiFoxp3+) or co-express KLRG1 (KLRG1+ Tregs) within viable CD45+CD3+CD4+ cells in the spleen (C) or Tumor (D). The proportions of CD8+ T cells were assessed against Tregs. (E) CD8: Treg ratios in the tumors of mice treated as indicated. Data is representative (A) or are mean ± SEM (E) of 5 mice per group. * indicates p-value < 0.05, ** p-value < 0.01, *** p-value < 0.001.

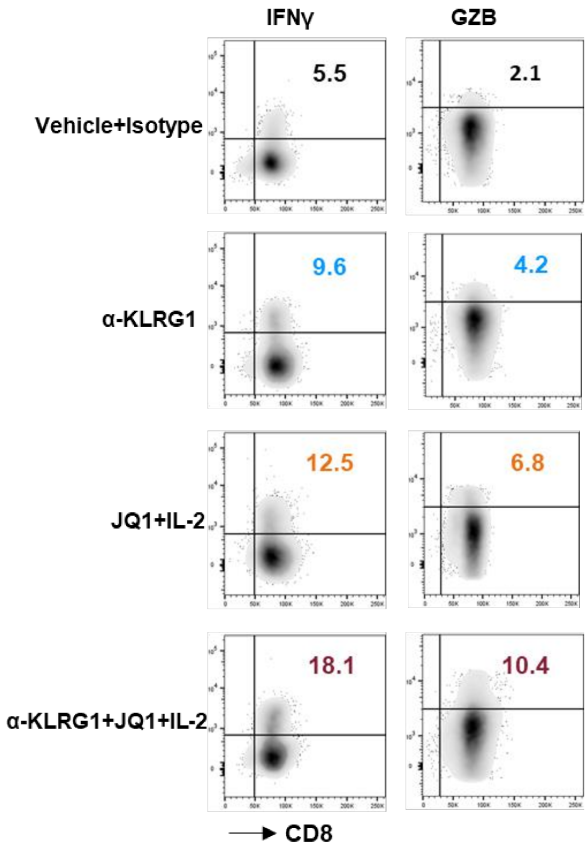

Fig. S10. Improved effector function of tumor-infiltrating CD8+ T cells upon Treg targeting and IL-2 supplementation. Mice with established B16-F10 tumors (25-35 mm^3) were treated with α-KLRG1 antibody and/or JQ1 plus IL-2 complex (IL-2C) and tumors were resected at clinical endpoints. Tumor-infiltrating CD45+CD3+ T cells were isolated from tumor cell suspensions and equivalent numbers stimulated for 6 hours with Cell Stimulation Cocktail plus protein transport inhibitor after which intracellular staining was conducted. Shown are representative plots for the proportion of gated CD8+ T cells that expressed IFN-γ (left) or Granzyme B (GZB; right) under each drug treatment condition as indicated. Data is representative of 5 mice per group.

Table 1.

Mouse

A

Antibodies	Antigen	Clone	Supplier
	Bax	bs-0127R	Bioss
FITC			
Percp-Cy5.5	CD8	53-6.7	Biolegend
	BTLA	6A6	Biolegend
APC	GZB	QA16A02	Biolegend
AF647			
AF700	Foxp3	FJK-16s	Invitrogen
	PD-1	29F.1A12	Biolegend
APC/Cy7	TIGIT	1G9	Biolegend
BV-421	TNF-α	MP6-XT22	Biolegend
BV605	CD45	30-F11	Biolegend
	CD4	RM4-5	Biolegend
BV650			
BV711	KLRG1	2F1/KLRG1	Biolegend
BV785	CD3	17A2	Biolegend
BUV395	CD25	PC61	BD Biosciences
BUV737	PD1	J43	BD Bioscience
	CTLA4	UC10-4B9	Biolegend
	IFNγ	XMG1.2	Invitrogen
PE	Bcl-2	BCL/10C4	Biolegend
PECF594			
PE-Dazzle 594			
PE-Cy7			
BUV805	GITR	DTA-1	BD Biosciences

Human

B

Antibodies	Antigen	Clone	Supplier
BUV805	CD45	H130	BD Biosciences
BUV661	CD3	UCHT1	BD Biosciences
AF700	CD4	SK3	BioLegend
PerCP/Cy5.5	CD8	SK1	BioLegend
BUV737	CD25	2A3	BD Biosciences
BUV395	CD127	HIL-7R-M21	BD Biosciences
PE/Dazzle 594	FOXP3	206D	BioLegend
BV605	TIGIT	A15153G	BioLegend
BV785	PD1	NAT105	BioLegend
PE/Cyanine 7	CTLA-4	L3D10	BioLegend